

Article

Synthesis of Green-Emitting (La,Gd)OBr:Tb³⁺ Phosphors

Sun Woog Kim, Kazuya Jyoko, Toshiyuki Masui and Nobuhito Imanaka *

Department of Applied Chemistry, Faculty of Engineering, Osaka University, 2-1 Yamadaoka, Suita, Osaka 565-0871, Japan; E-Mails: swkim@chem.eng.osaka-u.ac.jp (S.W.K.); kazuya@chem.eng.osaka-u.ac.jp (K.J.); masui@chem.eng.osaka-u.ac.jp (T.M.)

* Author to whom correspondence should be addressed; E-Mail: imanaka@chem.eng.osaka-u.ac.jp; Tel.: +81-6-6879-7352; Fax: +81-6-6879-7354.

Received: 29 December 2009; in revised form: 12 March 2010 / Accepted: 31 March 2010 /

Published: 1 April 2010

Abstract: Green-emitting phosphors based on lanthanum-gadolinium oxybromide were synthesized in a single phase form by the conventional solid state reaction method, and photoluminescence properties of them were characterized. The excitation peak wavelength of (La_{1-x}Gd_x)OBr:Tb³⁺ shifted to the shorter wavelength side with the increase in the crystal field around the Tb³⁺ ions by doping Gd³⁺ ions into the La³⁺ site, and, as a result, the green emission intensity was successfully enhanced. The maximum emission intensity was obtained for (La_{0.95}Gd_{0.05})OBr:5% Tb³⁺, where the relative emission intensity was 45% of that of a commercial green-emitting LaPO₄:Ce³⁺, Tb³⁺ phosphor.

Keywords: green-emitting phosphor; rare earth oxybromide; crystal field modification; solid state reaction

1. Introduction

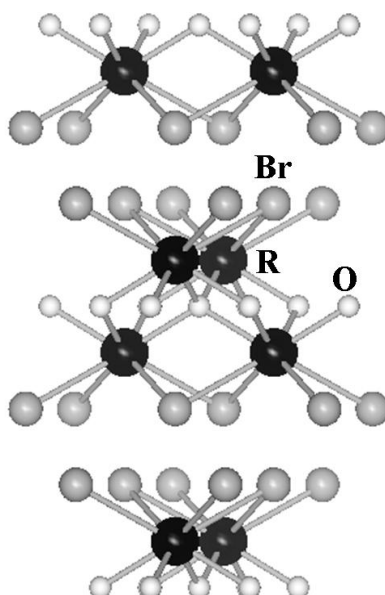
A number of materials activated by trivalent rare earth ions, which can exhibit light-emitting properties, have been widely used as phosphors. It is well known that some of the trivalent rare earth ions can show bright line spectra based on 4f-4f transitions, because the 4f-electrons are well shielded from the surroundings by the 5s and 5p orbitals. Among such rare earth ions, Tb³⁺ have been commonly recognized as a green activator due to the efficient emission originated from the ⁵D₄-⁷F_J (J = 6, 5, 4, and 3) transitions [1].

The luminescent properties of phosphors usually depend on the concentration of the activator ion in the host lattice. When the amount of the activator is in excess, the emission intensity is decreased generally due to the concentration quenching, because the decrease in the mean activator-activator distance often induces the non-radiative deactivation. This phenomenon is significantly related to the crystal structure of the host lattice of the phosphor. Therefore, many investigations have been devoted to search for new materials, which can avoid the concentration quenching, even if a large amount of the activator is doped in the host [2,3].

In our previous studies, we reported red- and green-emitting phosphors based on rare earth oxycarbonate [4–10], rare earth oxysulfate [11], and zirconium oxide phosphate [12]. These phosphors can show good fluorescent properties due to their layer structures. In these structures, energy transfer from an excited luminescent ion to another across the anion groups (*i.e.*, CO_3^{2-} , SO_4^{2-} , and PO_4^{3-} groups) is inhibited by the long distance. Accordingly, phosphors based on such layer structures should be resistant to concentration quenching.

In the present study, we have focused on tetragonal PbFCl-type rare earth oxybromide, ROBr (R = rare earths), as a host material of the phosphor. The PbFCl-type ROBr can form a layer structure similar to those of the phosphors previously studied in our laboratory, where the $(\text{RO})_n^{n+}$ layers (R = rare earths) are separated by bromide ions in the direction to the *c*-axis, as illustrated in Figure 1, in which the R^{3+} ions are surrounded by four O^{2-} and four Br^- ions with C_{4v} point site symmetry [13,14]. In the series of the rare earth oxybromides, LaOBr has the highest thermal stability [15], and general luminescent properties of the phosphors based on LaOBr activated by trivalent rare earth ions have been investigated by several researchers [16–30]. Among several rare earth activators, it has been suggested that terbium is the most effective activator to obtain high emission intensity by the investigation on the X-ray luminescence of LaOBr: R^{3+} [20]. However, there is no report focusing on the relative luminescent intensities in comparison with the commercially available phosphors under UV excitation.

Figure 1. Crystal structure of the tetragonal PbFCl-type ROBr (R = rare earths).



In this study, LaOBr:Tb³⁺ phosphors were synthesized and the photoluminescence properties of the prepared particles were investigated in detail and compared with those of the commercially available LaPO₄:Ce³⁺, Tb³⁺ phosphor. Furthermore, in order to further enhance the emission intensity of the LaOBr:Tb³⁺ phosphor, part of the La³⁺ ions in the LaOBr host lattice were substituted with smaller Gd³⁺ ions to enhance the crystal field around the Tb³⁺ ions.

2. Results and Discussion

The sample composition was analyzed by X-ray fluorescence analysis and it was confirmed that all samples were synthesized in each stoichiometric ratio as summarized in Table 1. X-ray powder diffraction (XRD) patterns for the (La_{1-x}Gd_x)OBr:5%Tb³⁺ (0 ≤ x ≤ 0.2) phosphor samples are shown in Figure 2. The XRD patterns of the samples with x ≤ 0.15 were identical to a single phase of tetragonal PbFCl-type rare earth oxybromide structure with high crystallinity, and there is no diffraction peak corresponding to any impurities in the patterns. On the other hand, an impurity phase corresponding to cubic Gd₂O₃ was observed in the sample with x = 0.2. A peak shift to higher diffraction angle is observed with the increase in the amount of Gd³⁺ in the host LaOBr lattice for the samples with x ≤ 0.15, because La³⁺ (ionic radius: 0.116 nm for 8 coordination) [31] sites in the host material is partially substituted with the smaller Gd³⁺ cation (ionic radius: 0.1053 nm for 8 coordination) [31]. Figure 3 depicts the effect of Gd³⁺ content on the (La_{1-x}Gd_x)OBr:5%Tb³⁺ lattice volume, which decreases monotonously with the increase in the Gd³⁺ content and becomes approximately constant at the Gd³⁺ concentration higher than x = 0.15. These results indicate that the smaller Gd³⁺ successfully substituted La³⁺ site in host LaOBr lattice in the samples with x ≤ 0.15, and the solid solution limit is at around 15 atom % Gd³⁺ replacement of the La³⁺ site in (La_{1-x}Gd_x)OBr:5%Tb³⁺.

Table 1. Theoretical and analyzed compositions of the samples.

Theoretical composition	Analyzed composition
LaOBr:5% Tb ³⁺	(La _{0.95} Tb _{0.05})OBr
(La _{0.95} Gd _{0.05})OBr:5% Tb ³⁺	(La _{0.9} Gd _{0.05} Tb _{0.05})OBr
(La _{0.9} Gd _{0.1})OBr:5% Tb ³⁺	(La _{0.84} Gd _{0.11} Tb _{0.05})OBr
(La _{0.85} Gd _{0.15})OBr:5% Tb ³⁺	(La _{0.79} Gd _{0.16} Tb _{0.05})OBr
(La _{0.8} Gd _{0.2})OBr:5% Tb ³⁺	(La _{0.76} Gd _{0.19} Tb _{0.05})OBr

Figure 4 depicts the excitation spectra for the emission at 543 nm in the (La_{1-x}Gd_x)OBr:5%Tb³⁺ (0 ≤ x ≤ 0.15) samples. The excitation spectra of all samples consist of strong broad bands from 230 to 275 nm, corresponding to the energy transition from the 4f⁸ to 4f⁷5d configuration of Tb³⁺. The peak wavelength in the excitation bands based on the 4f-5d transition of Tb³⁺ depends on the crystal field, which is affected by the lattice volume of the oxybromide phosphor. As summarized in Table 2, each 4f-5d transition band can be divided into three Gaussian peaks, where two peaks at the short-wavelength side correspond to the spin allowed 4f-5d transitions of Tb³⁺ and the other weak peak at the long-wavelength side corresponds to the spin forbidden transition of Tb³⁺ [3234]. The crystal field strength increases with increasing amount of Gd³⁺ substitution for La³⁺ in the oxybromide lattice,

because the average $\text{Tb}^{3+}\text{-O}^{2-}$ bond length becomes progressively shorter by the lattice shrinkage (Figure 3). The increase of the crystal field strength of O^{2-} around Tb^{3+} leads one of the spin allowed excitation bands to shift to shorter wavelength (higher energy), and the other one to longer wavelength (lower energy). As a result, the crystal field splitting between two spin-allowed components in Table 2 enhances with increasing the Gd^{3+} content. In addition, the energy separation between the spin-allowed and spin-forbidden component is about 6000 cm^{-1} , which basically agrees with the value reported previously [32,34].

Figure 2. XRD patterns for the $(\text{La}_{1-x}\text{Gd}_x)\text{OBr}:5\%\text{Tb}^{3+}$ ($0 \leq x \leq 0.2$) phosphors.

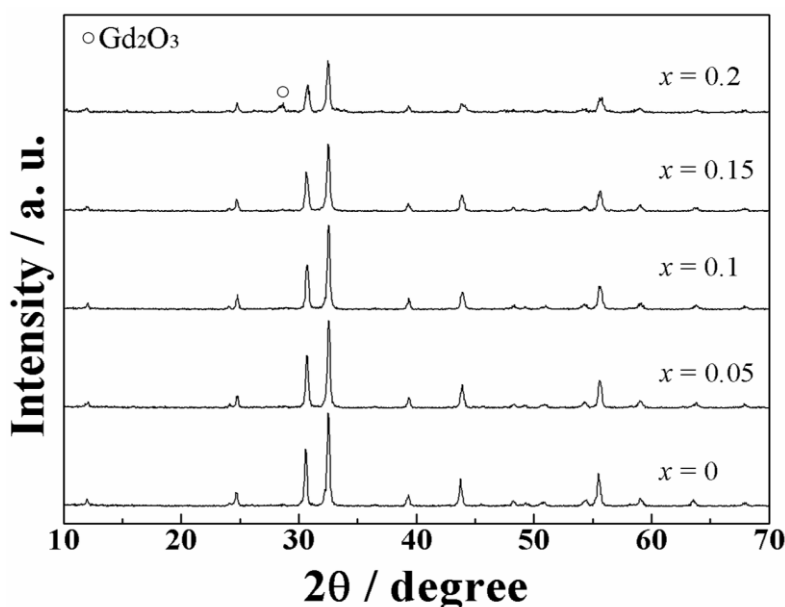


Figure 3. Dependence of the lattice volume on the concentration of Gd^{3+} in the $(\text{La}_{1-x}\text{Gd}_x)\text{OBr}:5\%\text{Tb}^{3+}$ ($0 \leq x \leq 0.2$) phosphors.

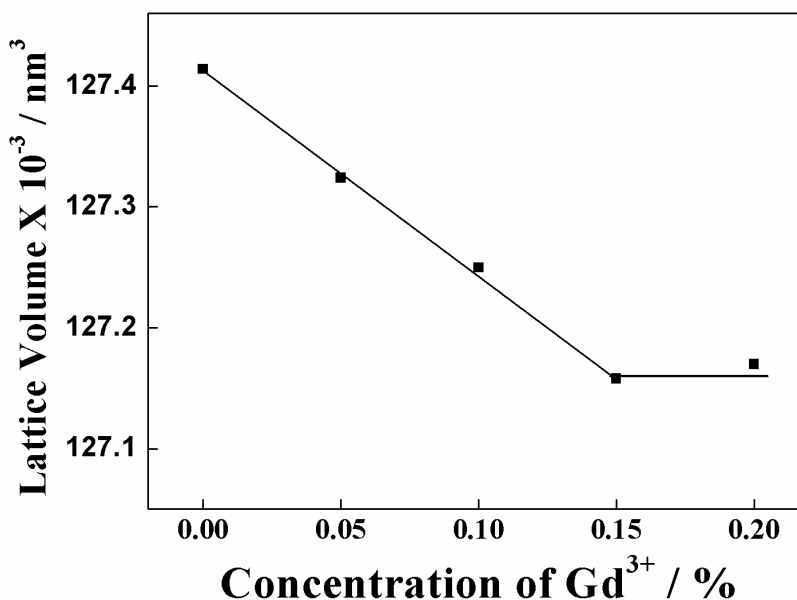


Figure 4. Excitation spectra of the $(\text{La}_{1-x}\text{Gd}_x)\text{OBr}:5\%\text{Tb}^{3+}$ phosphors; $x =$ (a) 0, (b) 0.05, (c) 0.10, and (d) 0.15.

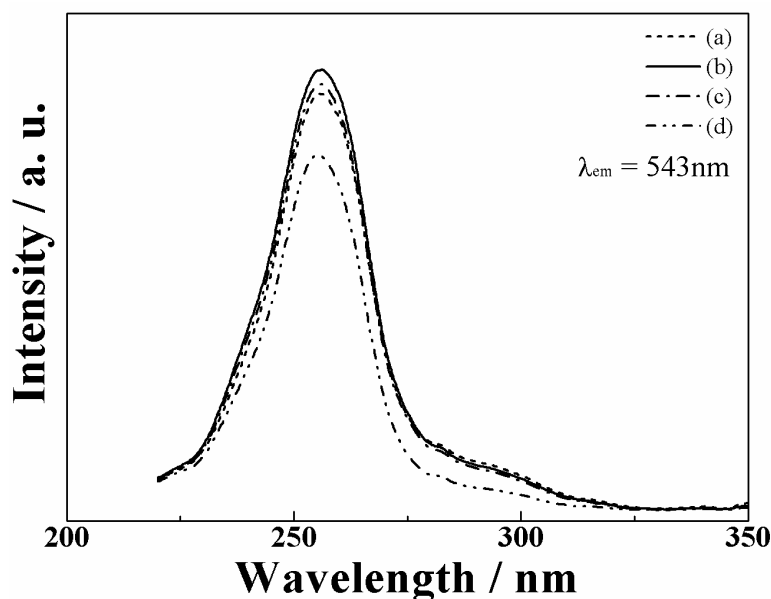


Table 2. Spectral data of Tb^{3+} in $(\text{La}_{1-x}\text{Gd}_x)\text{OBr}:5\%\text{Tb}^{3+}$ ($x = 0 - 0.15$).

	$x = 0$	$x = 0.05$	$x = 0.10$	$x = 0.15$
$4f^8-4f^75d$ (1) (nm)	243.9	243.4	242.8	242.1
$4f^8-4f^75d$ (2) (nm)	256.8	257.0	257.3	257.8
$4f^8-4f^75d$ (3) (nm)	282.9	283.6	284.3	284.8
Energy separation width = (1) – (3) (cm^{-1})	5652	5824	6012	6193

Figure 5 illustrates the emission spectra of the $(\text{La}_{1-x}\text{Gd}_x)\text{OBr}:5\%\text{Tb}^{3+}$ phosphors under excitation at 254 nm. The oxybromide phosphors exhibited a well-known characteristic Tb^{3+} emission and no self-activated emission was observed in the undoped samples. The emission peaks observed at 484, 543, 587 and 625 nm correspond to the transition from the $^5\text{D}_4$ excited level to the $^7\text{F}_6$, $^7\text{F}_5$, $^7\text{F}_4$, and $^7\text{F}_3$ ground levels of Tb^{3+} , respectively. In addition, the peak shape of all samples were identical with no spectral shift due to the introduction of Gd^{3+} into the $\text{LaOBr}:5\%\text{Tb}^{3+}$ lattice, because of the shielding effect of electrons in the 4f orbital by the outer 5s and 5p orbitals, whereby the crystal field has less influence.

Figure 6 presents the dependence of the emission intensity on the Gd^{3+} concentration in the $(\text{La}_{1-x}\text{Gd}_x)\text{OBr}:5\%\text{Tb}^{3+}$ ($0 \leq x \leq 0.15$) phosphors. Reproducible results were obtained for all samples and the standard deviation, which was evaluated by statistical processing of the reproductive experiments, was small. The emission intensity was successfully increased in the samples with $x = 0.05$ and 0.10, by the Gd^{3+} doping into the LaOBr lattice.

Figure 5. Emission spectra of the $(\text{La}_{1-x}\text{Gd}_x)\text{OBr}:5\%\text{Tb}^{3+}$ phosphors; $x =$ (a) 0, (b) 0.05, (c) 0.10, and (d) 0.15.

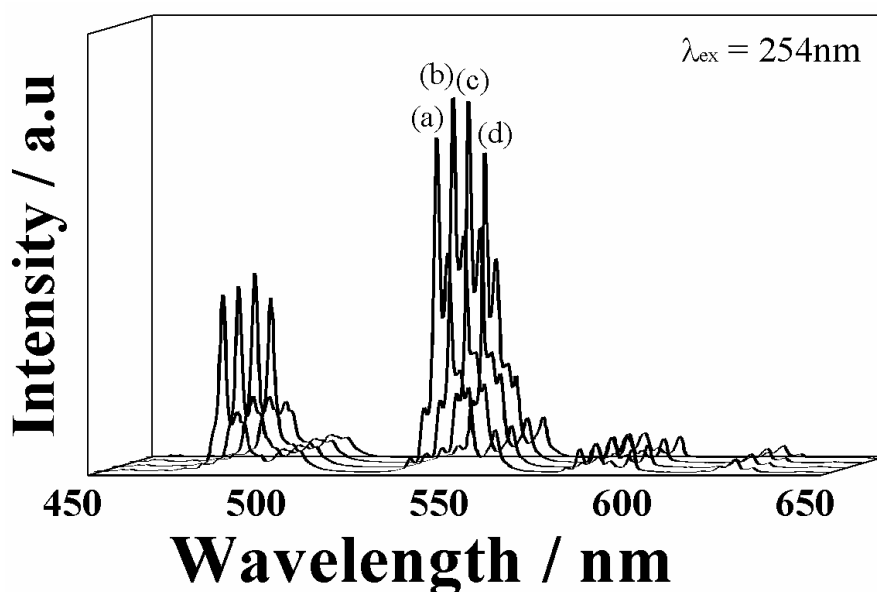
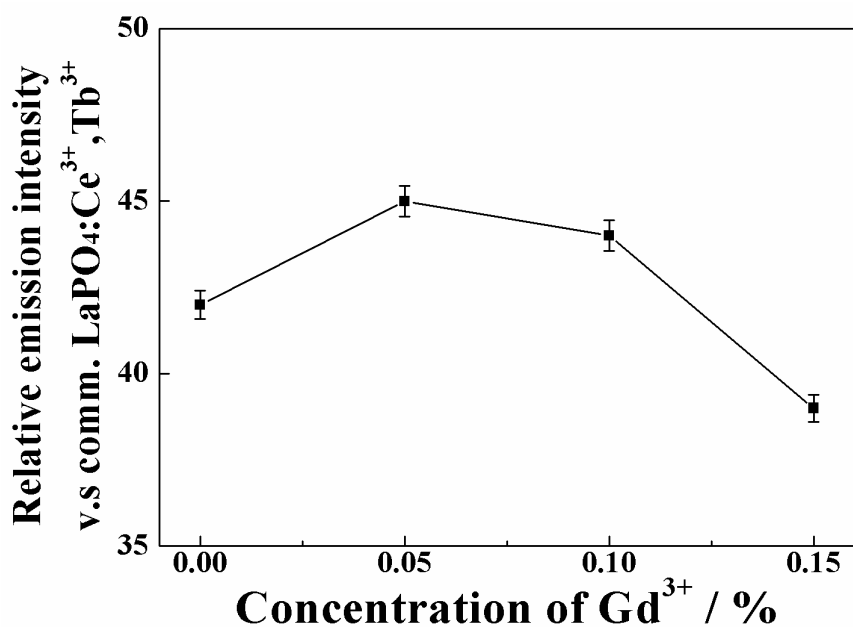


Figure 6. Dependence of the emission intensity on the Gd^{3+} concentration in the $(\text{La}_{1-x}\text{Gd}_x)\text{OBr}:5\%\text{Tb}^{3+}$ ($0 \leq x \leq 0.15$) phosphors. The excitation wavelength is 254 nm for both $(\text{La}_{1-x}\text{Gd}_x)\text{OBr}:5\%\text{Tb}^{3+}$ and $\text{LaPO}_4:\text{Ce}^{3+},\text{Tb}^{3+}$.



There are two possibilities for the reason why the emission intensity increased in the samples with $x = 0.05$ and 0.10 in $(\text{La}_{1-x}\text{Gd}_x)\text{OBr}:5\%\text{Tb}^{3+}$. First, the crystal field effect is suggested. The peak wavelength in the excitation spectra shifted to shorter wavelength side and became closer to the excitation wavelength of 254 nm by the increase in the crystal field. Secondly, the increase in the crystallinity of the phosphor also contributes to the enhancement of the emission intensity. The full width at half maximum (FWHM) of the XRD peaks in Figure 2 was estimated for each $(\text{La}_{1-x}\text{Gd}_x)\text{OBr}:5\%\text{Tb}^{3+}$.

$x\text{Gd}_x\text{)OBr:5\%Tb}^{3+}$ ($0 \leq x \leq 0.15$) phosphor, and the results are summarized in Table 3. The FWHM correlates with the crystallinity of the phosphors, which affects the excitation and emission properties. The FWHM obtained for the samples with $x = 0.05$ and 0.10 became smaller than that of LaOBr:5\%Tb^{3+} , indicating that the crystallinity was increased by the Gd^{3+} doping. On the contrary, the FWHM for $x = 0.15$ became larger than that of LaOBr:5\%Tb^{3+} . These results are consistent with the excitation and emission data shown in Figures 4, 5, and 6. In accordance with the FWHM width of the sample, the excitation and the emission intensities reach a maximum at $x = 0.05$ in $(\text{La}_{1-x}\text{Gd}_x)\text{OBr:5\%Tb}^{3+}$.

Table 3. The full width at half maximum (FWHM) of the X-ray diffraction peak from the (102) planes of the $(\text{La}_{1-x}\text{Gd}_x)\text{OBr:5\%Tb}^{3+}$ ($x = 0 - 0.15$) phosphors.

	$x = 0$	$x = 0.05$	$x = 0.10$	$x = 0.15$
FWHM (degree)	0.2531	0.2457	0.2457	0.2814

The excitation and the emission intensities of the sample with $x = 0.10$ were still higher than those of LaOBr:5\%Tb^{3+} . However, these intensities tend to decrease with the Gd^{3+} content beyond the optimum concentration. The decrease in both the excitation and the emission intensities is probably due to the imperfect atomic arrangement correlating with the FWHM expansion in the LaOBr host matrix, and the distortion in the host matrix leads to fluorescence quenching [35]. The ionic radius of Gd^{3+} is smaller than that of La^{3+} , so that the excess Gd^{3+} doping should introduce extra strain into the LaOBr lattice; therefore, emission quenching is expected beyond an optimum Gd^{3+} concentration by the decrease in the crystallinity of the phosphor.

Consequently, the maximum emission intensity was obtained at the composition of $(\text{La}_{0.95}\text{Gd}_{0.05})\text{OBr:5\%Tb}^{3+}$, where the relative emission intensity was 45% compared to that of a commercial $\text{LaPO}_4:\text{Ce}^{3+},\text{Tb}^{3+}$ lamp phosphor. Although the emission intensity of this phosphor is not sufficient in the present stage, improvement of the luminescence property can be expected by the optimization of the amount of Tb^{3+} ion as well as the preparation process such as flux treatment, which can eliminate surface defects of the phosphor effectively. In addition, it is necessary to improve chemical stability of the oxybromide phosphor for potential application because of low stability against water. Surface treatment with $\text{AlPO}_4/\text{Al}(\text{OH})_3$ with the additive MgSO_4 has been suggested as an effective way to improve the stability [36].

3. Experimental Section

The $(\text{La}_{1-x}\text{Gd}_x)\text{OBr:Tb}^{3+}$ ($0 \leq x \leq 0.2$) phosphors were synthesized by the conventional solid state reaction method. La_2O_3 , Gd_2O_3 , $\text{Tb}(\text{NO}_3)_3 \cdot 6\text{H}_2\text{O}$, and NH_4Br were mixed in a stoichiometric ratio using a mortar, in which the amount of Tb^{3+} in the phosphors was adjusted to be 5%. Then, the mixture was mechanically mixed using a planetary ball milling apparatus (Pulverisette 7, FRITSCHE GmbH) for 12 h. The homogenous mixture was calcined in a flow of pure N_2 gas at $900\text{ }^\circ\text{C}$ for 12 h. The precursor obtained was heated again in a flow of $2\%\text{H}_2\text{-98\%Ar}$ gas at $900\text{ }^\circ\text{C}$ for 6 h for the reduction of Tb^{4+} to Tb^{3+} .

The crystal structure of the samples was identified by X-ray powder diffraction (XRD; Rigaku Multiflex) analysis, and the sample composition was confirmed by X-ray fluorescence spectroscopy (Rigaku ZSX100e). Photoluminescence excitation and emission spectra were measured at room temperature with spectrofluorophotometer (Shimadzu RF-5300PC). The emission spectra were obtained for excitation at 254 nm, and the excitation spectra were recorded for the emission peak at 543 nm (5D_4 - 7F_5 transition of Tb^{3+}). The relative emission intensities of the $(La_{1-x}Gd_x)OBr:5\%Tb^{3+}$ ($0 \leq x \leq 0.2$) phosphors were estimated by comparing the integrated area of the emission peak at 543 nm with that of the commercial $LaPO_4:Ce^{3+},Tb^{3+}$ phosphor.

4. Conclusion

Green-emitting phosphors based on lanthanum-gadolinium oxybromide, $(La_{1-x}Gd_x)OBr:5\%Tb^{3+}$ ($0 \leq x \leq 0.2$) were synthesized by the conventional solid state reaction method. Oxybromide phosphors with tetragonal $PbFCl$ -type structure were obtained in a single phase having high crystallinity for the samples with $x \leq 0.15$. The photoluminescence spectra showed green emission from the 5D_4 excited level to the 7F_J ($J = 6, 5, 4,$ and 3) ground levels of Tb^{3+} . The photoluminescent intensity was increased by the Gd^{3+} doping and the emission reached the maximum intensity at $x = 0.05$ in $(La_{1-x}Gd_x)OBr:5\%Tb^{3+}$, where the relative emission intensity compared with that of the commercial $LaPO_4:Ce^{3+},Tb^{3+}$ phosphor was 45%.

Acknowledgements

The present work was supported by a Grant-in-Aid for Scientific Research No. 21750207 from the Ministry of the Education, Culture, Sports, Science and Technology of Japan.

References and Notes

1. Kang, Y.C.; Kim, E.J.; Lee, D.Y.; Park, H.D. High Brightness $LaPO_4:Ce,Tb$ Phosphor Particles with Spherical Shape. *J. Alloys Compd.* **2002**, *347*, 166–170.
2. Honma, T.; Toda, K.; Ye, Z.G.; Sato, M. Concentration Quenching of the Eu^{3+} Activated Luminescence in Some Layered Perovskites with Two Dimensional Arrangement. *J. Phys. Chem. Solids* **1998**, *59*, 1187–1193.
3. Wang, Z.; Liang, H.; Wang, Q.; Luo, L.; Gong, M. Luminescent Properties of Tb^{3+} Activated Double Molybdates and Tungstates. *Mater. Sci. Eng. B* **2009**, *164*, 120–123.
4. Tamura, S.; Koyabu, K.; Masui, T.; Imanaka, N. Lithium Carbonate Flux Effect on the Luminescence Properties of Europium-doped Lanthanum Oxycarbonate Phosphor. *Chem. Lett.* **2004**, *33*, 58–59.
5. Masui, T.; Koyabu, K.; Tamura, S.; Imanaka, N. Synthesis of a New Green-emitting Phosphor Based on Lanthanum Oxycarbonate ($La_2O_2CO_3$ -II). *J. Mater. Sci.* **2005**, *40*, 1421–1423.
6. Masui, T.; Mayama, Y.; Koyabu, K.; Imanaka, N. Synthesis of New Green-emitting $Gd_2O_2CO_3:Tb^{3+}$ Fine Particles with High Luminescence Intensities. *Chem. Lett.* **2005**, *34*, 1236–1237.

7. Koyabu, K.; Masui, T.; Tamura, S.; Imanaka, N. Synthesis of a New Phosphor Based on Rare Earth Oxycarbonate. *J. Alloys Compd.* **2006**, *408–412*, 867–870.
8. Koyabu, K.; Mayama, Y.; Masui, T.; Imanaka, N. Synthesis of New Green Emitting Phosphor Based on Rare Earth Oxycarbonate. *J. Alloys Compd.* **2006**, *418*, 230–233.
9. Mayama, Y.; Koyabu, K.; Masui, T.; Tamura, S.; Imanaka, N. Synthesis of New Red Emitting Phosphor Based on Rare Earth Oxycarbonate. *J. Alloys Compd.* **2006**, *418*, 243–246.
10. Mayama, Y.; Masui, T.; Koyabu, K.; Imanaka, N. Enhancement of the Luminescent Intensity of the Green Emitting $\text{Gd}_2\text{O}_2\text{CO}_3\text{:Tb}$ Phosphor. *J. Alloys Compd.* **2008**, *451*, 132–135.
11. Kim, S.W.; Masui, T.; Imanaka, N. Synthesis of Red-emitting Phosphors Based on Gadolinium Oxysulfate by a Flux Method. *Electrochemistry* **2009**, *77*, 611–613.
12. Kim, S.W.; Masui, T.; Matsushita, H.; Imanaka, N. Synthesis of New Green-emitting Phosphor Based on Zirconium Oxide Phosphate. *Chem. Lett.* **2009**, *38*, 1100–1101.
13. Haeuseler, H.; Jung, M. Single Crystal Growth and Structure of LaOBr and SmOBr. *Mater. Res. Bull.* **1986**, *21*, 1291–1294.
14. Hölsä, J.; Porcher, P. Crystal Field Effects in REOBr:Eu³⁺. *J. Chem. Phys.* **1982**, *76*, 2790–2797.
15. Hölsä, J.; Leskelä, M.; Niinistö, L. Thermal Stability of Rare Earth Oxybromides. *Themochim. Acta* **1980**, *35*, 79–83.
16. Li, Y.M.; Guillen, F.; Fouassier, C.; Hagenmuller, P. Comparative Study of Sensitization of the Luminescence of Trivalent Rare Earth Ions by Ce in LaOBr. *J. Electrochem. Soc.* **1985**, *132*, 717–721.
17. Wang, D.; Zhang, W.; Yin, M. Fluorescence Spectroscopy of Er³⁺:LaOBr Prepared by NH₄Br Solid State Reaction. *Opt. Mater.* **2004**, *27*, 605–608.
18. Wang, D.; Guo, Y.; Zhang, E.; Chao, X.; Yu, L.; Luo, J.; Zhang, W.; Yin, M. Synthesis and NIR-to-violet, Blue, Green, Red Upconversion Fluorescence of Er³⁺:LaOBr. *J. Alloys Compd.* **2005**, *397*, 1–4.
19. Guo, H. Two- and Three-photon Upconversion of LaOBr:Er³⁺. *Opt. Mater.* **2007**, *29*, 1840–1843.
20. Starick, D.; Golovkova, S.I.; Gurvic, A.M.; Herzog, G. Investigations on the X-ray Luminescence of LaOBr:RE³⁺ Phosphors. *J. Lumin.* **1988**, *40–41*, 199–200.
21. Wang, Q.; Bulou, A. Influence of Hydrostatic Pressure and Interatomic Distance upon the Energy Levels Scheme of Eu³⁺ in REOBr (RE = La, Gd or Y). *Solid State Commun.* **1995**, *94*, 309–315.
22. Rambabu, U.; Khanna, P.K.; Rao, I.C.; Buddhudu, S. Fluorescence Spectra of Eu³⁺-doped Lanthanide Oxybromide-based Powder Phosphors. *Mater. Lett.* **1998**, *34*, 269–274.
23. Reddy, K.R.; Aruna, V.; Balaji, T. Annapurna, K.; Buddhudu, S. Photoluminescence Spectra of LaOBr:Eu³⁺ Powder Phosphors. *Mater. Chem. Phys.* **1998**, *52*, 157–160.
24. Hölsä, J.; Leskelä, M.; Niinistö, L. Concentration Quenching of Tb³⁺ Luminescence in LaOBr and Gs₂O₂S Phosphors. *Mater. Res. Bull.* **1979**, *14*, 1403–1409.
25. Hölsä, J.; Leskelä, M.; Niinistö, L. Sensitization of Tb³⁺ Luminescence with Ce³⁺ in LaOBr:Tb³⁺,Ce³⁺. *J. Solid State Chem.* **1981**, *37*, 267–270.
26. Zhao, F.T.; Cao, L.Y.; Xu, X.R. The Energy Transfer Between Ce³⁺ and Tb³⁺ Ions in LaOBr:Ce³⁺,Tb³⁺. *J. Electrochem. Soc.* **1987**, *134*, 3186–3190.
27. Starick, D.; Lange, W.; Herzog, G. Investigations on the Thermoluminescence of LaOBr:Tb³⁺ Phosphors. *J. Thermal Anal.* **1988**, *33*, 889–894.

28. Ronda, C.R.; Bechtel, H.; Kynast, U.; Welker, T. The Degradation Behavior of LaOBr:Tb Under Cathode-ray Excitation. *J. Appl. Phys.* **1994**, *75*, 4636–4641.
29. Yang, J.; Gong, J.; Fan, H.; Yang, L. The Structure and Luminescence Characteristics of LaOBr:Tb³⁺(Dy³⁺). *J. Mater. Sci.* **2005**, *40*, 3725–3728.
30. Mazurak, Z.; Garcia, A.; Fouassier, C. Luminescence Spectra and Crystal Field Analysis of LaOBr Doped with Tm³⁺. *J. Phys.: Condens. Matter* **1994**, *6*, 2031–2037.
31. Shannon, R.D. Revised Effective Ionic Radii and Systematic Studies of Interatomic Distances in Halides and Chalcogenides. *Acta. Cryst.* **1976**, *A32*, 751–767.
32. Jia, P.Y.; Lin, J.; Han, X.M.; Yu, M. Pechini Sol-gel Deposition and Luminescence Properties of Y₃Al_{5-x}Gd_xO₁₂:Ln³⁺ (Ln³⁺ = Eu³⁺, Ce³⁺, Tb³⁺; 0 ≤ x ≤ 5) Thin Films. *Thin Solid Films* **2005**, *483*, 122–129.
33. Blasse, G.; Bril, A. Investigations of Tb³⁺-Activated Phosphors. *Philips Res. Rep.* **1967**, *22*, 481–504.
34. Pieterse, L.; Reid, M.F.; Burdick, G.W.; Meijerink, A. 4f→4fⁿ⁻¹5d¹ Transitions of the Heavy Lanthanides: Experiment and Theory, *Phys. Rev. B* **2002**, *65*, 045114.
35. Chong, M.K.; Pita, K.; Kam, C.H. Photoluminescence of Sol-gel-derived Y₂O₃:Eu³⁺ Thin-film Phosphors with Mg²⁺ and Al³⁺ Co-doping. *Appl. Phys. A* **2004**, *79*, 433–437.
36. Sun, J.; Du, X.; Kyotani, T.; Tomita, A. Effect of Surface Treatment on Stability of Lanthanum Oxide Bromide Phosphor. *React. Solids* **1989**, *7*, 331–342.

© 2010 by the authors; licensee Molecular Diversity Preservation International, Basel, Switzerland. This article is an open-access article distributed under the terms and conditions of the Creative Commons Attribution license (<http://creativecommons.org/licenses/by/3.0/>).